VTT Technical Research Centre of Finland

Thermodynamic affinity in constrained free-energy systems

Koukkari, Pertti; Pajarre, Risto; Kangas, Petteri

Published in:
Monatshefte für Chemie

DOI:
10.1007/s00706-017-2095-5

Published: 01/01/2018

Document Version
Early version, also known as pre-print

This is a post-peer-review, pre-copyedit version of an article published in Monatshefte für Chemie - Chemical Monthly. The final authenticated version is available online at: http://dx.doi.org10.1007/s00706-017-2095-5

Thermodynamic Affinity in Constrained Free Energy Systems

Pertti Koukkari[1] ● Risto Pajarre[1] ● Petteri Kangas[1]

Received: ……/Accepted …

Abstract Affinity is the generic measure of the deviation of a state from stable equilibrium. Affinity, as introduced by de Donder, is a thermodynamic state property defined in terms of p, T and system composition during the course of a chemical change. When incorporating reaction kinetic constraints to minimization of Gibbs energy of a multiphase system, affinity can be followed in terms of the extents of the constrained reactions. This property then becomes calculated in terms of the constraint potentials received as additional Lagrange multipliers in the minimization routine. Thus, received affinities are consistent with the respective values calculated from the chemical potentials of the reactants and products of the constrained reactions and their limiting behaviour corresponds to that defined for both

stationary and stable equilibrium states. The intermediate affinities can be used in the respective reaction rate calculations, or as input parameters, to define the local chemical equilibrium set by known reaction kinetic constraints. Thus, they become a useful concept in modelling reactive processes.

Keywords Thermodynamics ● Computational chemistry ● Local thermodynamic equilibrium ● CFE

✉ Pertti Koukkari
Pertti.koukkari@vtt.fi
[1] VTT Technical Research Centre of Finland Ltd, Finland
[1] Institute of Chemistry, University of Albertville, Albertville, Australia
[2] Institute of Chemistry, affiliation of second author

Introduction

Local and partial chemical equilibria, including paraequilibria systems and reactive non-equilibrium systems constrained by extent of reaction can be calculated within the Gibbs energy minimizing programs. The Constrained Gibbs Free Energy (CFE) method makes use of complementary conservation conditions for selected immaterial properties in addition to the conservation of molar amounts of the physical system components [1–5]. The CFE method can be used to introduce slow reaction kinetics to multicomponent and multiphase Gibbsian calculations, thus providing a series of timely intermediate states which are constrained by the extent of these reactions [6, 7]. In this respect, the CFE is somewhat parallel with the Rate Controlled Chemical Equilibrium (RCCE) technique applied to multicomponent combustion systems in homogeneous gas phase [8, 9], which has been increasingly used recently to reduce extensive mechanistic calculations of turbulent flames [10–12]. The solution of the calculation then is a differential-algebraic procedure, which combines the necessary constraint (either static or dynamic) with the linearized min(G) problem. The chemical potentials of the system components are solved Lagrange multipliers. As the complementary constraints are introduced via immaterial system components, the solution of the constrained systems will include additional Lagrange multipliers, each of those representing another physically

meaningful potential for the said system. Additional Lagrange multipliers are typically adjacent to physical functions which may be deciphered as thermodynamic work when CFE methodology is applied. In non-equilibrium conditions, when additional constraints are applied for extents of a reaction, the Gibbsian solution of the constrained multi-component system will provide the non-zero affinity as a combination of the additional Lagrange multipliers and the stoichiometric relations used for the (reaction) constraints [5].

The concept of affinity as a thermodynamic state property $A \equiv A(p, T, n_1, n_2, \ldots, n_N)$ was introduced by de Donder [13]. Following the original definition, affinity can be regarded as a generic measure (or 'driving force') of the deviation of an arbitrary thermochemical state from equilibrium [14]. However, most frequently thermodynamic affinity is linked with the time-dependent extent of chemical reactions [$\xi=\xi(t)$]. The well-known properties defined by de Donder are zero affinity and $d\xi/dt$ =0 at equilibrium and $A \neq 0$ and dξ/dt =0 for metastable states. In irreversible thermodynamics, affinity has been widely applied as a useful concept which can be coupled with generalized forces when studying linear phenomena (for example Haase [15] Kondepudi and Prigogine [16] and Kjelstrup et al.[17]). While non-equilibrium affinities of elementary reactions can be directly utilized in reaction rate terms, they also have been extensively used in

developing rate models in non-linear irreversible thermodynamics [18, 19]. Following such principles, e.g. Vuddagiri & al [20] used dynamic modelling of reaction pathways on Gibbs energy surfaces (for reactor optimization) and Lems et al. [21] pursued finding optimum conditions for chemical energy conversion with coupled affinities. In biochemistry, affinities are used in developing models for metabolic networks by using non-equilibrium models [22, 23]. Further, in the field of non-equilibrium thermodynamics Niven [24] introduces an alternative formulation of the maximum entropy principle which leads to a free-energy-like potential to be minimized in steady state conditions. The affinity appears as one of the thermodynamic forces in the local potential function, which reduces to Gibbs free energy in the equilibrium system. Ross et al. [25] specify the affinity-dependent potential with reference values either at stationary or stable equilibrium states. Instead, in research connected directly with multi-component multiphase computational thermodynamics, the concept of affinity is but sparsely used. Smith and Missen [26] in their seminal book on this topic lay the fundamental equations in both constituent and component formalisms and, as referred above, Hillert [14] presents a more universal affinity concept to represent the driving force of thermochemical transformations. Pope (see Ren et al. [11]) and his co-workers have introduced the ‘constraint potentials’ while using the rate-controlled chemical equilibrium (RCCE)

method when modelling combustion and turbulent flames as related with the affinity of the non-equilibrium reactions. While one of the authors [27] developed the novel Ratemix method, it was proclaimed that the affinity of each intermediate state can be received from the constrained Gibbsian calculations. In the later development of the Constrained Gibbs free energy minimization method (CFE), it has become possible to make use of the affinity-related reaction rates directly in time-dependent simulations of multi-component and multi-phase chemical change, either by using the incremental affinities as part of the reaction rate data within the sequential calculation [28] or by applying them as input parameters to define the composition of the respective super-equilibrium [29] and local chemical equilibrium [30].

In the following, an extension of the theory presented by Smith and Missen for global equilibrium states to constrained non-equilibrium systems is pursued. Further, it is shown that the affinity received as the combination of the additional Lagrange multipliers (the constraint potentials) is consistent with the conventional thermodynamic affinity definition.

Results and Discussion

Multicomponent equilibrium systems in terms of component potentials

As the system will consist of N constituents and NC system components, the condition for minimizing the Gibbs energy is

$$\min G(\boldsymbol{n}) \quad s.t. \quad \sum_{k=1}^{N} c_{jk} n_k = b_j \qquad j = 1,2,\dots,NC \tag{1}$$

where j indicates the components of the system and, respectively, k constituents (species). c_{jk} refers to the stoichiometric coefficient between component j and constituent k. n_k is the molar amount of constituent k while b_j is the molar amount component j. The Lagrange function, L, for the minimization problem is

$$L = G - \sum_{j=1}^{NC} \pi_j \left[\sum_{k=1}^{N} c_{jk} n_k - b_j \right] \tag{2}$$

where $\boldsymbol{\pi}$ is a vector of NC unknown Lagrange multipliers ($\boldsymbol{\pi}^{\mathbf{T}} = \pi_1, \pi_2, \dots, \pi_{NC}$) and the given conditions provide the set of (N+NC) equations for the same number of unknowns ($n_1, n_2, \dots, n_N; \pi_1, \pi_2, \dots, \pi_{NC}$) to be solved, as follows

$$\left(\frac{\partial L}{\partial n_k}\right)_{\pi, n_{i \neq k}} = \mu_k - \sum_{j=1}^{NC} c_{jk}\, \pi_j = 0 \qquad (n_k \geq 0) \tag{3}$$

$$\left(\frac{\partial L}{\partial \pi_j}\right)_{\boldsymbol{n}, \pi_{i \neq j}} = b_j - \sum_{k=1}^{N} c_{jk}\, n_k = 0 \qquad (n_k \geq 0) \tag{4}$$

These equalities provide the necessary conditions for chemical equilibrium in the multicomponent system. As c_{jk} are dimensionless factors representing

the stoichiometric relations defining the constituents of the system in terms of their components it is obvious from (3) that the Lagrange multipliers (π_j) become solved as the chemical potentials of the system components. This feature is of advantage when additional constraints connected with the advancements of selected reactions are applied, as discussed later. In the following, the component formalism is applied for the affinity state function in both equilibrium and kinetically constrained non-equilibrium multicomponent systems.

Introduction of advancement constraints to the stoichiometric component formalism

The extents of reactions are used as additional constraining conditions analogous to those defined for the basic mass balance of equation (4). For a single chemical reaction written in the form

$$w_A A + w_B B \Leftrightarrow w_C C + w_D D \tag{a.1}$$

the extent of reaction is defined as

$$d\xi = -\frac{dn_A}{w_A} = -\frac{dn_B}{w_B} = \frac{dn_C}{w_C} = \frac{dn_D}{w_D} \equiv \frac{dn_k}{\upsilon_k} \tag{5}$$

where stoichiometric coefficient υ_i equals w_i for products and $-w_i$ for reactants. In a system with multiple possible reactions, it is in general impossible to define the change in extent of any individual reaction of the

form (a.1) based on the change of system composition, if not also the other linearly independent reactions forming a basis spanning the reaction space are first defined. When they are, one can solve for $\mathbf{d\xi}$ the equation

$$\mathbf{dn} = \boldsymbol{\upsilon} \mathbf{d\xi} \tag{6}$$

where $\mathbf{dn}$ is the vector of changes of molar amounts of the N constituents in the system, $\mathbf{d\xi}$ a vector of changes in extents of the R specified reactions, and $\boldsymbol{\upsilon}$ is a $N \times R$ matrix of stoichiometric coefficients of the reaction vectors spanning the reaction space.

The relation between the reaction matrix ($\boldsymbol{\upsilon}$) and stoichiometry of the multicomponent system is given with the matrix equation

$$\mathbf{C}\boldsymbol{\upsilon} = \mathbf{0} \tag{7}$$

where $\mathbf{C}$ is a NC×N matrix of stoichiometric coefficients between the N constituents and NC components (NC=rank($\boldsymbol{\upsilon}$)), forming a link between the system stoichiometry and the reactions allowed by it [26, 31].

While the connection between the stoichiometric conservation and reaction matrixes in the equilibrium system was presented by Eq. (7), any kinetic constraints set for the possible reactions that cause the system to develop towards some other state than full equilibrium will lead to a new matrix equation

$$\mathbf{C}'\boldsymbol{\upsilon}' = \mathbf{0} \tag{8}$$

where $\boldsymbol{\upsilon}'$ is a $N \times R'$ matrix ($R' < R$) made of the reduced reaction set and $\mathbf{C}'$ is the corresponding $NC' \times N$ matrix ($NC' = NC + R - R' \equiv NC + C$, where C is the number of added constraints) of stoichiometric coefficients for the new augmented matrix of stoichiometric coefficients. Each reduction on the number of linearly independent reactions allowed to freely equilibrate corresponds to an additional stoichiometric constraint, or a row in the $\mathbf{C}$ matrix, that is linearly independent of the previously defined reaction kinetic constraints or other component balances. In a multispecies constrained equilibrium system, the independent net reactions that lead to changes in system composition are practically defined by using the following relation (9)

$$d\xi_r \equiv \sum_k c_{NC+r,k} dn_k = db_{NC+r} \tag{9}$$

where $c_{NC+r,k}$ is the matrix element in the extended matrix $\mathbf{C}'$, where the $NC + r^{\text{th}}$ row defines the constraint related to the reaction constraint and db_{NC+r} is the incremental change in the amount of the corresponding element in the augmented component vector. The matrix form corresponding to equation (9) is

$$\mathbf{d\xi} = \mathbf{C}''\mathbf{dn} = \mathbf{db}'' \tag{10}$$

where $\mathbf{C}''$ is the $C \times N$ submatrix forming the lower part of $\mathbf{C}'$. Intuitively, that the extent of a reaction is defined following equations (9) or (10) on the

basis of a constraining components rather than individual species is most easily understood in a system which has extensive partial equilibria both with species in the reactant and product side of the reaction. A typical example is the change in oxidation state of sulphur species in aqueous solution. A constraining component is then applied for each sulphur valence state not in equilibrium with each other and the changes in oxidation reaction extent is readily expressed by the change in the amount of these components.

If the number of these defined reaction constraints equals R, so that no unconstrained linearly independent reactions remain ($R' = 0$), $\mathbf{C}''$ in equation (10) can be replaced with $\mathbf{C}'$, and $\mathbf{d\xi}$ with $\mathbf{d\xi}'$, where the first $N - R$ components of the $\mathbf{d\xi}'$ vector equal zero, and the last R components are the same as in $\mathbf{d\xi}$.

$$\mathbf{d\xi}' = \mathbf{C}'\mathbf{dn} \tag{11}$$

Matrix $\mathbf{C}'$ has linearly independent rows and thus it is invertible. The matrix $(\mathbf{C}')^{-\mathbf{1}}$ contains coefficients for reaction like transformations for the species. In each transformation, the amount of one of the components is increased by one, while the amounts of other components are kept constant. In matrix form this can be stated as

$$(\mathbf{C}')^{-\mathbf{1}}\mathbf{C}' = \mathbf{I} \tag{12}$$

Multiplying equation (11) by $(\mathbf{C}')^{-\mathbf{1}}$ one obtains

$$(\mathbf{C}')^{-\mathbf{1}}\mathbf{d\xi}' = \mathbf{dn} \quad (13)$$

The first NC transformations are connected with the normal component balances and the respective changes of the advancement vector $\mathbf{d\xi}'$ are zero. The remaining reactions are the ones constrained by equation (10). The elements of the last R columns of matrix $(\mathbf{C}')^{-\mathbf{1}}$ equal matrix $\boldsymbol{\upsilon}$ and the last R values respectively vector $\mathbf{d\xi}$ in equation (10), and thus the definition in equation (10) is formally equivalent with the one in equation (6).

The significance of the matrix transformation is that the constraints due to extents of reactions introduced as new components in matrix $\mathbf{C}'$ can directly be applied as additional conditions in free energy minimization calculations. As an example, for a system with the following species H_2, CH_4, C_2H_4, C_2H_6, C_3H_8 , $N = 5$ and $NC = 2$, so that it is possible to define a maximum of three independent constrained reactions using the formalism of equation (9), corresponding, for example, to the following $\mathbf{C}'$ matrix, where the first two rows refer to the elements C and H and the last three to the added constraints. The constraints set here are of arbitrary nature for the schematic example, though the first ($c(1)$) and last one ($c(3)$) obviously are linked to the amounts of species C_3H_8 and C_2H_6, respectively. For the regular mass balances to remain valid, the new components $c(1) - c(3)$ should be defined to have zero mass.

$$C' = \begin{matrix} H_2 & CH_4 & C_2H_4 & C_2H_6 & C_3H_8 \\ \end{matrix} \begin{matrix} \\ \\ \\ \\ \\ \end{matrix} \begin{matrix} \\ \\ \\ \\ \\ \end{matrix}$$
$$\begin{bmatrix} 0 & 1 & 2 & 2 & 3 \\ 2 & 4 & 4 & 6 & 8 \\ 0 & 0 & 0 & 0 & 1 \\ 1 & 0 & -1 & 0 & 0 \\ 0 & 0 & 0 & 1 & 0 \end{bmatrix} \begin{matrix} C \\ H \\ c(1) \\ c(2) \\ c(3) \end{matrix} \quad (14)$$

By inspection or by linear algebra one can derive

$$(C')^{-1} = \begin{bmatrix} 2 & -0.5 & -2 & 2 & -1 \\ -3 & 1 & 1 & -2 & 0 \\ 2 & -0.5 & -2 & 1 & -1 \\ 0 & 0 & 0 & 0 & 1 \\ 0 & 0 & 1 & 0 & 0 \end{bmatrix} \begin{matrix} H_2 \\ CH_4 \\ C_2H_4 \\ C_2H_6 \\ C_3H_8 \end{matrix} \quad (15)$$

where the last three columns give in the traditional reaction equation format the following three rate-constrained reactions compatible with both equations (6) and (10). Advancement of each of the reactions (b.1)–(b.3) correspond to addition of one mole of constraining components $c(1)-c(3)$, respectively.

$$2H_2 + 2C_2H_4 \Leftrightarrow C_3H_8 + CH_4 \quad \text{(b.1)}$$

$$2CH_4 \Leftrightarrow C_2H_4 + 2H_2 \quad \text{(b.2)}$$

$$C_2H_4 + H_2 \Leftrightarrow C_2H_6 \quad \text{(b.3)}$$

However, the three reaction constraints, $c(1)-c(3)$ given as rows in matrix (14) are also unambiguously defined individually, while the reaction equation format (b.1–b3) is properly defined only for a full set of independent equilibrium or non-equilibrium reactions.

Applying reaction advancements into a constrained system based on mechanistic reaction kinetics

When a rate for a reaction of the form (a.1) is applied for the constrained system based on an assumed or known reaction mechanism, the changes in the amounts of constraining components depend on the relative stoichiometries of the applied reaction (a.1) and constraint (9). The reaction of the generic stoichiometry (a.1) is here considered as an actual process whereby the species in the system are transformed to other species with a finite rate, even if this transformation violates one or more of the added reaction constraints (reactions that do not violate any of the constraints would always remain in equilibrium). The change in amounts of the constraining components are calculated based on equation

$$db_{NC+r} = \sum_k c_{NC+r,k} dn_k = \sum_k c_{NC+r,k} \upsilon_{k,i}\, d\xi_i \qquad (16)$$

For the most practical application of this relation, a new column to the $\mathbf{C}'$can be defined as a new virtual feed phase for the system. The definition of the virtual feed phase is done in such way that addition of one mole of the virtual phase corresponds to a one molar unit positive change in reaction i advancement. If the reaction (depending on conditions) can proceed in either the forward or reverse direction, to avoid negative feed amounts, two virtual phases can be applied, with the second having stoichiometric coefficients

with opposite signs. During calculation it is possible to include and exclude these virtual phases if needed. By defining the virtual phases to have zero standard chemical potential at all temperatures (enthalpy, entropy and heat capacity are zero), they can be added without affecting the energy balance of the system [1, 5, 28].

$$\mathbf{c}' = \begin{matrix} \\ \\ \\ \\ \\ \\ \end{matrix} \overset{\begin{matrix} N\ species \end{matrix} \quad + \quad \begin{matrix} K\ mechanistic\ reactions \cdot 2 \end{matrix}}{\begin{bmatrix} c_{1,1} & \cdots & c_{1,N} & 0 & \cdots & 0 \\ \vdots & \ddots & \vdots & \vdots & \ddots & \vdots \\ c_{NC,1} & \cdots & c_{NC,N} & 0 & \cdots & 0 \\ c_{NC+1,1} & \cdots & c_{NC+1,N} & \sum_k c_{NC+1,k}\upsilon_{k,1} & \cdots & -\sum_k c_{NC+1,k}\upsilon_{k,K} \\ \vdots & \ddots & \vdots & \vdots & \ddots & \vdots \\ c_{NC+C,1} & \cdots & c_{NC+C,N} & \sum_k c_{NC+C,k}\upsilon_{k,1} & \cdots & -\sum_k c_{NC+C,k}\upsilon_{k,K} \end{bmatrix} \begin{matrix} \\ \\ \\ \\ \\ \\ \end{matrix} \overset{\begin{matrix} NC \\ components \\ + \\ C \\ reaction \\ constraints \end{matrix}}{\ } \tag{17}$$

As an example, adding virtual phases for the rate of the reaction

$$C_2H_4 + CH_4 \Leftrightarrow C_3H_8 \tag{c.1}$$

in to the system defined by the matrix (14) would result in a new matrix

$$C' = \begin{matrix} \\ \\ \\ \\ \\ \end{matrix} \overset{\begin{matrix} H_2 & CH_4 & C_2H_4 & C_2H_6 & C_3H_8 & r^+ & r^- \end{matrix}}{\begin{bmatrix} 0 & 1 & 2 & 2 & 3 & 0 & 0 \\ 2 & 4 & 4 & 6 & 8 & 0 & 0 \\ 0 & 0 & 0 & 0 & 1 & 1 & -1 \\ 1 & 0 & -1 & 0 & 0 & 1 & -1 \\ 0 & 0 & 0 & 1 & 0 & 0 & 0 \end{bmatrix} \begin{matrix} C \\ H \\ c(1) \\ c(2) \\ c(3) \end{matrix} \tag{18}$$

where the last two columns, labelled r^+ and r^-, are for the virtual phases for the forward and reverse reactions following (c.1). Formally, the reaction (c.1) as a part of the Constrained Free Energy model is now

$$C_2H_4 + CH_4 + r^+ \Leftrightarrow C_3H_8 \tag{c.1}$$

or on a component basis

$$\big(2C + 4H - c(2)\big) + (C + 4H) + \big(c(1) + c(2)\big) \Leftrightarrow\ 3C + 8H + c(1) \qquad \text{(c.1)}$$

Reaction affinity in the component formalism

The thermodynamic affinity of a chemical reaction of the form (a.1) is defined as

$$\mathbb{A}_r \ \equiv\ -\sum_{k_r} \upsilon_{k,r}\,\mu_k \tag{19}$$

Thus, for a spontaneous non-equilibrium reaction $\mathbb{A}_r > 0$, while for a reaction in equilibrium $\mathbb{A}_r = 0$. Applying Eqs. (3) and (19), affinity is obtained based on chemical potentials of components

$$\mathbb{A}_r = -\sum_{k=1}^{N} \upsilon_{k,r}\,\mu_k = \ -\sum_{k=1}^{N} \upsilon_{k,r} \sum_{j=1}^{NC'} c_{j,k}\,\pi_j \tag{20}$$

This can be rearranged to (Smith and Missen [26], p. 48):

$$\begin{aligned} \mathbb{A}_r = \ -\sum_{k=1}^{N}\sum_{j=1}^{NC'} \upsilon_{k,r} c_{j,k}\,\pi_j = \ -\sum_{j=1}^{NC'} \pi_j \sum_{k=1}^{N} \upsilon_{k,r} c_{j,k} \\ = -\sum_{j=1}^{NC'} \left(\frac{\partial G}{\partial b_j}\right)_{b_{i\neq j}} \sum_{k=1}^{N} \upsilon_{k,r} c_{j,k} \end{aligned} \tag{21}$$

as $\pi_j = \frac{\partial G}{\partial b_j}$. For the stoichiometric equilibrium system

$$\sum_{k=1}^{N} \upsilon_{k,r} c_{j,k} \ = 0; \quad r = 1,2,\dots,R \tag{22}$$

and thus, affinity, as derived from the multicomponent Gibbsian approach, is then zero and Eq. (21) is in agreement with the conventional definition.

However, with the constraining components included ($NC< j \leq NC+C$), this condition is not valid and a non-zero value for the affinity is received.

The affinity of a single constrained reaction j, as defined by Eq. (9) in a non-equilibrium system, is directly related to the chemical potential of the corresponding component.

$$\mathbb{A}_{\mathrm{r}} = -\left(\frac{\partial G}{\partial \xi_r}\right)_{T,P,b_i \xi_{r\prime \neq r}} = -\left(\frac{\partial G}{\partial b_{r+NC}}\right)_{T,P,b_i \xi_{r\prime \neq r}} = -\pi_{r+NC} \qquad (23)$$

where b_i is used for the amount of any of the components $b_1 \ldots b_{NC}$ in the system. For a general reaction of some other stoichiometry, the affinity is obtained as a linear combination of the constraint components (note that $NC' = NC + C$)

$$\mathbb{A}_r = -\sum_k \upsilon_{k,r}\mu_k = -\sum_{j=NC+1}^{NC+C} \pi_j \upsilon_{j,,r} \qquad (24)$$

where the condition (22) was again used. $\nu_{k,r}$ is the stoichiometric coefficient between the reaction r and constituent (species) k, so that the affinity of a reaction not in the original constrained basis set (10) is obtained as a linear combination of affinities of the base set reactions. Obviously, the two expressions for the affinity from (21) and (24) remain equivalent. The affinity from Eq. (24) also equals the chemical potential of the virtual species as defined in matrix (17).

The right-hand side of Eq. (24) epitomizes the division of the calculated affinity to the contributions of the physical and virtual components in the non-equilibrium condition. The equilibrium stipulation (zero affinity) for these constraints will yet follow from the inequality conditions of the Lagrange method used in the Gibbs energy minimization procedure. The inequality (Kuhn-Tucker) conditions (written for pure substances *k*) in the Lagrange method are as follows

$$\mu_k^* - \sum_{j=1}^{NC'} c_{jk}\,\pi_j = 0 \qquad (n_k > 0) \tag{25}$$

$$\mu_k^* - \sum_{j=1}^{NC'} c_{jk}\,\pi_j > 0 \qquad (n_k = 0) \tag{26}$$

where the asterisk denotes a pure (invariant) substance as a system constituent (phase). When the combination of virtual constituents and virtual components are being used to constrain the extent of the reaction in the minimization procedure, the above conditions are written for the virtual phases adjacent to reactants and products in each constrained reaction (*r*). Then, as the standard chemical potential is by definition zero for the virtual phases ($\mu_k^* \equiv 0$), it follows from (26) that $\sum_{j=1}^{NC'} c_{jk}\pi_j \neq 0$ for non-equilibrium situations (no virtual phase present in the system, $n_k = 0$). Respectively, from (26) $\sum_{j=1}^{NC'} c_{jk}\pi_j \equiv 0$ when equilibrium has been reached

and the calculation finds the virtual phase appearing as stabile in the Gibbs energy minimum system.

As setting the chemical potential of such a phase by adjusting its feed amount is also a well-established feature in free energy minimizers [5, 32, 33], the affinity of the corresponding reaction can further be adjusted to a desired value for a kinetically constrained reaction. As a specific case, setting a zero value for a chemical potential of the virtual phase in such target calculation corresponds to (partial) equilibrium in respect to that reaction.

With (25) the Eq. (26) remains formally analogous with Eqs. (19) and (22). The non-equilibrium affinity is then obtained in terms of the stoichiometric content of the virtual system components in the constrained reaction. When equilibrium is reached as the limiting case, the condition (24) brings $\mathbb{A}_r$ to zero. Thus, while applying the matrix extension to calculate kinetically constrained reaction multicomponent systems, the procedure remains consistent with the conventional definitions of the affinity.

Example cases

Systems with one constrained reaction

As first examples, two simple systems with one constrained reaction are considered. The first one, homogeneous gas-phase oxidation of sulphur dioxide (SO_2) to sulphur trioxide (SO_3), is well-known for its industrial significance. The reaction is typically performed by mixing sulphur dioxide

with air at a pressure slightly higher than atmospheric, and is passed through a catalyst converter, containing a number of layers of catalyst. For our purposes the reaction is yet assumed to obey a simple rate law as given in Table 1. The system also consists merely of the three gaseous constituents O_2, SO_2 and SO_3. The respective matrix description is given in Eq. (27) with constraint matrix elements set for the oxidation product SO_3.

$$C' = \begin{matrix} O_2 & SO_2 & SO_3 & r^+ & r^- \end{matrix} \begin{bmatrix} 0 & 1 & 1 & 0 & 0 \\ 2 & 2 & 3 & 0 & 0 \\ 0 & 0 & 1 & 1 & -1 \end{bmatrix} \begin{matrix} S \\ O \\ c \end{matrix} \tag{27}$$

The second simple example is the oxidation of gaseous titanium(IV)chloride ($TiCl_4$) to solid titanium dioxide (TiO_2). In this system, a number of side reactions including the dissociation of chlorine and formation of titanium oxychlorides may take place (e.g. Koukkari and Niemelä [34], West et al.[35]). The extensively simplified stoichiometry matrix is given in Eq. (28), with constraint elements set on reactant $TiCl_4$.

$$C' = \begin{matrix} O_2 & TiCl_4 & TiCl_3 & TiOCl_2 & Cl_2 & Cl & ClO & TiO_2 & r^+ & r^+ \end{matrix} \begin{bmatrix} 2 & 0 & 0 & 1 & 0 & 0 & 1 & 2 & 0 & 0 \\ 0 & 4 & 3 & 2 & 2 & 1 & 1 & 0 & 0 & 0 \\ 0 & 1 & 1 & 1 & 0 & 0 & 0 & 1 & 0 & 0 \\ 0 & -1 & 0 & 0 & 0 & 0 & 0 & 0 & 1 & -1 \end{bmatrix} \begin{matrix} O \\ Cl \\ Ti \\ c \end{matrix} \tag{28}$$

With the constraint set for only one reactant in the system, a number of side reactions will be allowed toward reaching mutual equilibrium. Such reactions include, e.g.

$$TiCl_4 + M \leftrightarrow TiCl_3 + Cl + M \quad \text{(d.1)}$$

$$Cl_2 \leftrightarrow 2Cl \quad \text{(d.2)}$$

$$Cl_2 + O_2 \leftrightarrow 2ClO \quad \text{(d.3)}$$

$$TiCl_3 + O_2 \leftrightarrow TiOCl_2 + ClO \quad \text{(d.4)}$$

In (d.1) M denotes any gaseous molecule. With additional $TiCl_n$ radicals and various Ti-oxychloride species the list can be continued to several dozens of reactions [34, 35][1]. Considering the arduous compilation of the mechanism with a great number of reactions with rather inaccurate rate data, it has been proposed to use local chemical equilibrium (LCE) assumption [6, 27]. Here the global reaction rate measured for the decay of $TiCl_4$ reactant in the oxidation system is applied for describing the great number of (elementary) side reactions when constructing a model for the $TiCl_4$ burner [6, 27]. Due to the considerable enthalpy effects of, e.g. Cl_2 dissociation, the validity of the LCE assumption also could be ascertained with measured temperature and heat transfer data, but from a pilot reactor also from the actual industrial production lines [34, 36].

The rate data for the SO_2 and $TiCl_4$ oxidation reactions is presented in Table 1. The extent of SO_2 oxidation was calculated for the isothermal homogenous system. The affinity received as the potential of the immaterial

[1] For example, West et al. list 51 reactions including (i) thermal decomposition, which initiates the radical reaction chain; (ii) radical abstraction of Cl and disproportionation; (iii) oxidation; and (iv) dimerization forming a $Ti_2O_xCl_y$ species.

component has been compared with the molar Gibbs energy change of the reaction ($\Delta_r G$). The system initial conditions are 0.01 mol SO_3, 20 mol SO_2, 24 mol O_2. The reaction is assumed isothermal at 400 °C and 101 kPa (Fig. 1). The respective isothermal $TiCl_4$ oxidation system (Fig. 2) consists of 1.0 mol $TiCl_4$ and 1.1 mol O_2 at 1360 °C. The non-isothermal system (Fig. 3) is calculated for an atmospheric plug flow reactor with feed rates O_2 4.0 mol s^{-1} (1600 °C) and $TiCl_4$ 3.54 mol s^{-1} (600 °C). The reaction is assumed to proceed after ideal mixing of the reactants in a plug flow reactor, with the overall reaction rate received from the Arrhenius equation as presented in Table 1. As for the heat transfer model and calculated temperature profiles of the plug flow reactor, the reader is referred to earlier work (see e.g. Koukkari et al. [36]). The affinities of both reactions were determined from the constraint potentials (received as the Lagrange multipliers of the respective constraining components in the matrixes (27) and (28) compared with the respective $\Delta_r G$ values calculated from the molar Gibbs energies of the reactants and products (as defined in the reaction equations of Table 1).

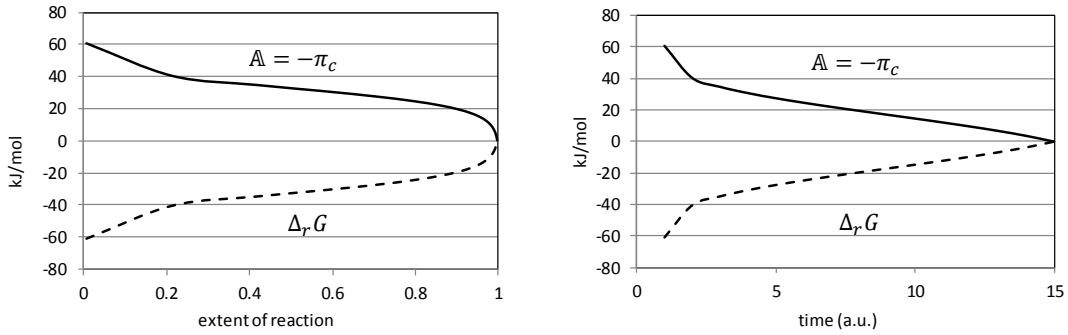

Fig. 1 The constraint potential affinities and $\Delta_r G$ values for the SO_2 oxidation system.

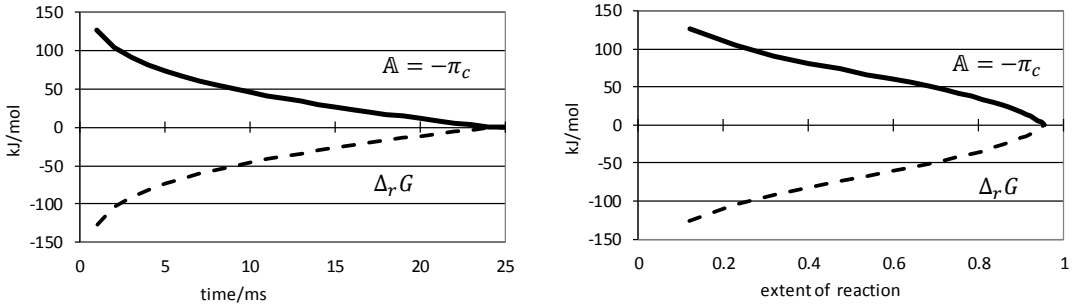

Fig. 2 The constraint potential affinities and $\Delta_r G$ values for the isothermal $TiCl_4$ oxidation system.

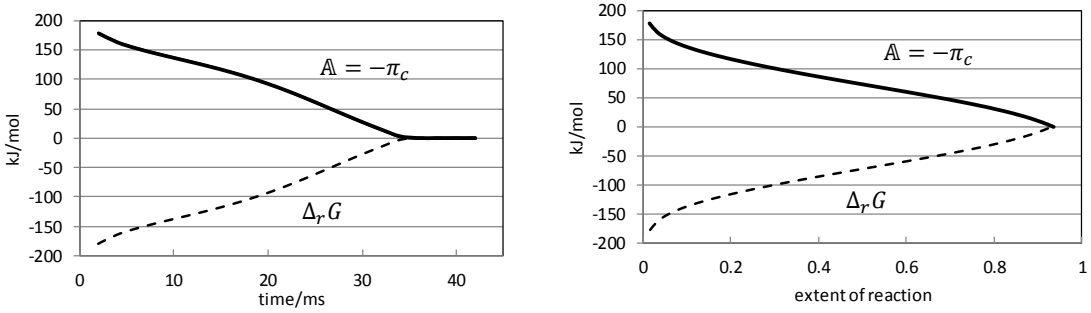

Fig. 3 The constraint potential affinities and $\Delta_r G$ values for the non-isothermal $TiCl_4$ oxidation system.

Table 1. The rate data for the SO_2 and $TiCl_4$ oxidation reactions.

Reaction	ΔH^o kJ · mol^{-1}	ΔG^o kJ · mol^{-1}	Rate equation	E_a kJ · mol^{-1}	A s^{-1}	A' (dm^3 · mol^{-1})^{½}s^{-1}
$SO_2 + 0.5O_2 \rightarrow SO_3$	-98.9	-35.5	$\frac{d[SO_3]}{dt} = k[O_2][SO_2]$	31.0	12.07	
$TiCl_4 + O_2 \rightarrow TiO_2 + 2Cl_2$	-175.4 (1000 °C)	-104.1 (1000 °C)	$\frac{d[TiCL_4]}{dt} = -\left(k + k'\sqrt{[O_2]}\right)[TiCl_4]$	85.0	8.26E4	1.4E5

The constraint potential affinities and $\Delta_r G$ values are depicted in Figures 1–3. The full symmetry is obvious following Eq. (23). The reaction extents are plotted on a normalized basis on the x-axis $0 \leq \xi/\xi_{max} \leq 1$ on the x-axis, where the limiting values correspond to those of fully unreacted system and to a system that has proceeded to stoichiometric completion.

Homogeneous stationary state system with two constrained reactions

In this example, a homogeneous gas phase system is again considered. The transient formation of nitric oxide emission in combustion flames have been extensively studied both experimentally and with modelling techniques including mechanistic kinetics [37] CFE [29] and RCCE [9]. In what follows, a reaction-constrained free-energy model is presented for carbon monoxide combustion in dry air. In addition, for the necessary reaction rate constraints a steady state assumption for oxygen radicals has been included.

For this simple case without hydrogen, the system and the matrix for stoichiometric coefficients $\mathbf{C^T}$ can be presented as

$$\mathbf{C^T} = \begin{array}{c} \begin{matrix} C & N & O \end{matrix} \\ \begin{bmatrix} 1 & 0 & 0 \\ 2 & 0 & 0 \\ 1 & 1 & 0 \\ 1 & 0 & 1 \\ 1 & 0 & 2 \\ 0 & 1 & 0 \\ 0 & 2 & 0 \\ 0 & 2 & 1 \\ 0 & 2 & 0 \\ 1 & 1 & 1 \\ 0 & 1 & 1 \\ 0 & 1 & 2 \\ 0 & 1 & 3 \\ 0 & 0 & 1 \\ 0 & 0 & 2 \end{bmatrix} \end{array} \begin{matrix} C \\ C_2N_2 \\ CN \\ CO \\ CO_2 \\ N \\ N_2 \\ N_2O \\ NCN \\ NCO \\ NO \\ NO_2 \\ NO_3 \\ O \\ O_2 \end{matrix} \tag{29}$$

Thermal NO emissions in high-temperature post-flame conditions can be described with the Zeldovich mechanism [38] described by Eqs. e.1 and 3.2. However, during the oxidation of hydrocarbons the radical over-shoot rapidly increases the NO emissions, which cannot be modelled with the Zeldovich mechanism alone. Thus, this simplified model is extended with the description of carbon monoxide oxidation and oxygen radical build-up (Eqs. e.3 and e.4).

$$N_2 + O \rightarrow N + NO \tag{e.1}$$

$$N + O_2 \rightarrow NO + O \tag{e.2}$$

$$CO + O_2 \rightarrow CO_2 + O \quad \text{(e.3)}$$

$$CO + O + M \rightarrow CO_2 + M \quad \text{(e.4)}$$

For the model, it was assumed that the constrained net reactions applied to the amounts of species NO, CO, O, so that these species are not allowed to freely equilibrate with any other species in the system. The stoichiometric matrix with these constraints added, $\mathbf{C'^T}$, is

$$\mathbf{C'^T} = \begin{array}{c} \begin{matrix} C & N & O & c(NO) & c(CO) & c(O) \end{matrix} \\ \begin{bmatrix} 1 & 0 & 0 & 0 & 0 & 0 \\ 2 & 0 & 0 & 0 & 0 & 0 \\ 1 & 1 & 0 & 0 & 0 & 0 \\ 1 & 0 & 1 & 0 & 1 & 0 \\ 1 & 0 & 2 & 0 & 0 & 0 \\ 0 & 1 & 0 & 0 & 0 & 0 \\ 0 & 2 & 0 & 0 & 0 & 0 \\ 0 & 2 & 1 & 0 & 0 & 0 \\ 0 & 2 & 0 & 0 & 0 & 0 \\ 1 & 1 & 1 & 0 & 0 & 0 \\ 0 & 1 & 1 & 1 & 0 & 0 \\ 0 & 1 & 2 & 0 & 0 & 0 \\ 0 & 1 & 3 & 0 & 0 & 0 \\ 0 & 0 & 1 & 0 & 0 & 1 \\ 0 & 0 & 2 & 0 & 0 & 0 \end{bmatrix} \end{array} \begin{array}{l} C \\ C_2N_2 \\ CN \\ CO \\ CO_2 \\ N \\ N_2 \\ N_2O \\ NCN \\ NCO \\ NO \\ NO_2 \\ NO_3 \\ O \\ O_2 \end{array} \quad (30)$$

When NO emission is considered, the reaction (e.1) is immediately followed by reaction (e.2) and the rate of formation of NO is given in Eq. (31). The oxidation of CO is described as the sum of reactions (e.3) and (e.4) and rate Eq. (32) is applied. For clarity, the respective rate constants are indexed as k_1, k_3 and k_4, respectively.

$$r_{NO} = 2k_1[N_2][O] \tag{31}$$

$$r_{CO} = -k_3[CO][O_2] - k_4[CO][O][M] \tag{32}$$

The changes in reaction advancements are calculated stepwise for time step $t_i \rightarrow t_{i+1}$

$$\Delta\xi_j = \Delta b_{M+j} = \int_{t_i}^{t_i+1} r_j dt \approx r_j(t_i)(t_{i+1} - t_i) \tag{33}$$

The effect of the reverse reaction rates can be estimated by the method described by Koukkari, et al. [28], where it is assumed that the effect is similar to one with an elementary reaction.

$$\frac{\mathrm{d}\xi_\mathrm{j}}{\mathrm{dt}} = \mathrm{r_j} = \mathrm{k_j}\left(1\text{-}\mathrm{e}^{-\frac{\mathrm{A_j}}{\mathrm{RT}}}\right) + \Pi_{\mathrm{reactants}}(\mathrm{a_k})^{|\nu_\mathrm{k}|} \tag{34}$$

$$= \mathrm{k_j}\left(1\text{-}\frac{\mathrm{Q_j}}{\mathrm{K_j}}\right)\Pi_{\mathrm{reactants}}(\mathrm{a_k})^{|\nu_\mathrm{k}|}$$

so that

$$r_j = r_j^0\ \left(1 - \frac{Q_j}{K_j}\right) = r_j^0\left(1 - e^{-\frac{\mathbb{A}_j}{RT}}\right) \tag{35}$$

where K_j is the equilibrium constant and Q_j the reaction quotient for reaction j and $\mathbb{A}_j$ its affinity and r_j^0, the rate of reaction far from equilibrium is taken as given by, e.g. Eqs. (31) and (32). As a numerical simplification, when the difference of rates of reactions (e.3) and (e.4) is estimated to be less than 10% of the rate of reaction (e.3), the O radical concentration is estimated by

the steady-state approximation (Eq. (36), using the respective indices for K_j and Q_j).

$$[O] = k_3 k_4^{-1} \left(1 - \frac{Q_3}{K_3}\right)\left(1 - \frac{Q_4}{K_4}\right)^{-1} [O_2][M]^{-1} \tag{36}$$

The O radical concentration following the steady state approximation (36) can be either set explicitly

$$b_{O^*}(t_{i+1}) = k_3 k_4^{-1} \left(1 - \frac{Q_3}{K_3}\right)\left(1 - \frac{Q_4}{K_4}\right)^{-1} ([O_2][M]^{-1})\Big|_{t_i} V \tag{37}$$

or implicitly by setting a corresponding deviation for the oxygen dissociation equilibrium. With K_O and Q_O defined as the equilibrium constant and reaction quotient for the dissociation reaction and $\mathbb{A}_O$ as the corresponding affinity.

$$\frac{1}{2} O_2 \leftrightarrow O \tag{e.5}$$

the deviation of oxygen dissociation from equilibrium can be expressed by

$$\begin{aligned} \frac{Q_0}{K_O} = e^{-\left(\frac{\mathbb{A}_O}{RT}\right)} = e^{\frac{\pi_{O^*}}{RT}} &= \frac{[O]}{[O_2]} \frac{\sqrt{x(O_2)}}{K_o} \\ &= \frac{1}{[M]} \frac{k_3}{k_4} \frac{\left(1 - \frac{Q_3}{K_3}\right)}{\left(1 - \frac{Q_4}{K_4}\right)} \frac{\sqrt{x(O_2)}}{K_o} \end{aligned} \tag{38}$$

Concentrations and mole fractions at the current time step t_x are utilized together with reaction and equilibrium constants for calculating the chemical

potential or affinity at t_{x+1}. A stoichiometric matrix with virtual phases used for adjusting reaction advancement, corresponding to the sum of reactions (e.1) and (e.2) (formation of NO), reaction (e.3) and reaction (e.4) is

$$\mathbf{C'^{T}} = \begin{array}{c} \begin{matrix} C & N & O & c(NO) & c(CO) & c(O) \end{matrix} \\ \left[\begin{matrix} 1 & 0 & 0 & 0 & 0 & 0 \\ 2 & 2 & 0 & 0 & 0 & 0 \\ 1 & 1 & 0 & 0 & 0 & 0 \\ 1 & 0 & 1 & 0 & 1 & 0 \\ 1 & 0 & 2 & 0 & 0 & 0 \\ 0 & 1 & 0 & 0 & 0 & 0 \\ 0 & 2 & 0 & 0 & 0 & 0 \\ 0 & 2 & 1 & 0 & 0 & 0 \\ 1 & 2 & 0 & 0 & 0 & 0 \\ 1 & 1 & 1 & 0 & 0 & 0 \\ 0 & 1 & 1 & 1 & 0 & 0 \\ 0 & 1 & 2 & 0 & 0 & 0 \\ 0 & 1 & 3 & 0 & 0 & 0 \\ 0 & 0 & 1 & 0 & 0 & 1 \\ 0 & 0 & 2 & 0 & 0 & 0 \\ 0 & 0 & 0 & 2 & 0 & 0 \\ 0 & 0 & 0 & -2 & 0 & 0 \\ 0 & 0 & 0 & 0 & -1 & 1 \\ 0 & 0 & 0 & 0 & 1 & -1 \\ 0 & 0 & 0 & 0 & -1 & -1 \\ 0 & 0 & 0 & 0 & 1 & 1 \end{matrix}\right] \end{array} \begin{matrix} C \\ C_2N_2 \\ CN \\ CO \\ CO_2 \\ N \\ N_2 \\ N_2O \\ NCN \\ NCO \\ NO \\ NO_2 \\ NO_3 \\ O \\ O_2 \\ r_{1+2}^{+} \\ r_{1+2}^{-} \\ r_{3}^{+} \\ r_{3}^{-} \\ r_{4}^{+} \\ r_{4}^{-} \end{matrix} \tag{39}$$

In Fig. 4 the calculation result with CFE is compared with the respective DKM (Zeldovich) approach. Fig. 5 shows the $\mathbb{A}_r$-evolution for reactions (e.1), (e.3) and (e.4) ($\mathbb{A}_1$, $\mathbb{A}_3$ and $\mathbb{A}_4$, respectively) during the course of the reaction time. Within the given time span, reaction (e.4) is approaching

equilibrium, while the affinity for reaction (e.1) indicates the stationary condition for oxygen radicals.

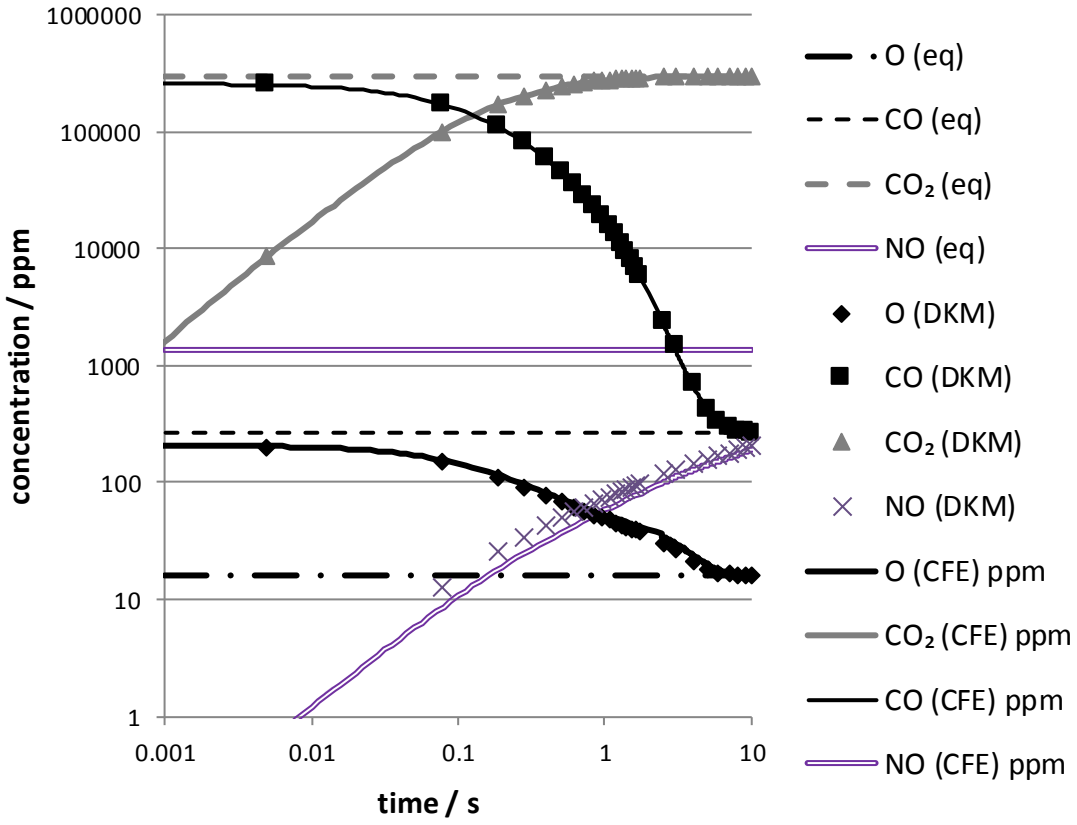

Fig. 4 Comparison of the CFE and DKM calculation results for the NO formation model.

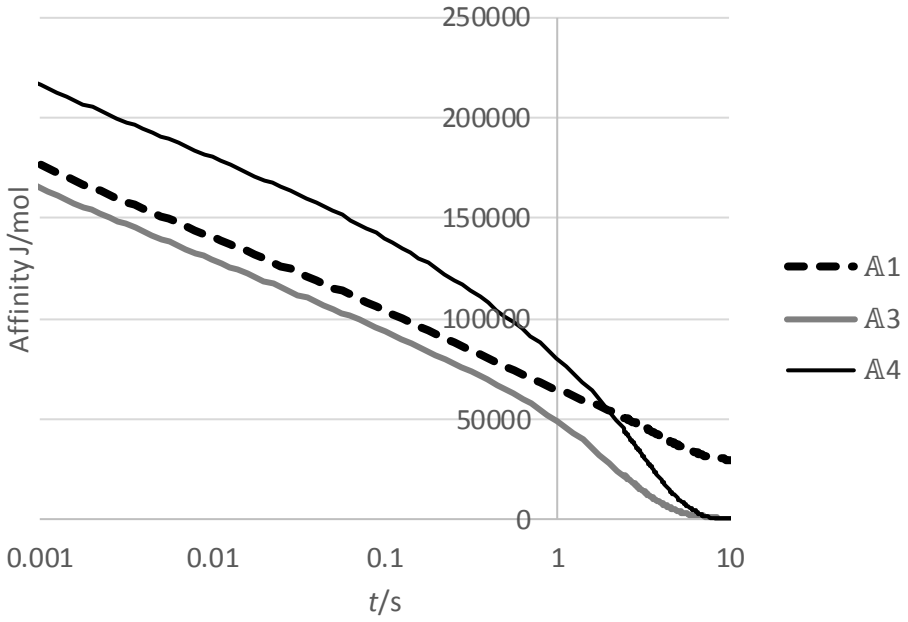

Fig. 5 Evolution of reaction affinities during the NO formation model.

A multiphase aqueous system with two constrained reactions

As an example of a slightly more complex system, a model for $CaCO_3$ precipitation from aqueous lime milk solution was constructed. The experimental system consists of a tubular reactor, to which CO_2-gas is first injected at ca 3 bar of pressure, followed by the feed of lime milk as aqueous $Ca(OH)_2$ slurry. With a close to stoichiometric feed of CO_2 and $Ca(OH)_2$ the reaction is instantaneous producing precipitated calcium carbonate and its progress can be followed in the reactor, e.g. by direct pH-measurement. Assuming ideal mixing and plug flow, a 1-dimensional model for the system was constructed and validated against the measured pH-values, which will vary from the original near neutral to pH ~ 12 at maximum and finally close

to neutral again when all the reactants have been consumed [28]. The slow reactions were assumed to be the absorption of the CO_2 from the gas to the aqueous phase and, respectively, the formation of precipitated $CaCO_3$ in the dynamic multiphase model. The multicomponent system with constraints is then as described in the $\mathbf{C^T}$ matrix below:

$$\mathbf{C'^T} = \begin{array}{c} \begin{matrix} N & O & C & H & Ca & EA & c(CO_2) & c(CaCO_3) \end{matrix} \\ \begin{bmatrix} 2 & 0 & 0 & 0 & 0 & 0 & 0 & 0 \\ 0 & 2 & 0 & 0 & 0 & 0 & 0 & 0 \\ 0 & 2 & 1 & 0 & 0 & 0 & 1 & 0 \\ 0 & 1 & 0 & 2 & 0 & 0 & 0 & 0 \\ 0 & 1 & 0 & 2 & 0 & 0 & 0 & 0 \\ 0 & 0 & 0 & 1 & 0 & -1 & 0 & 0 \\ 0 & 1 & 0 & 1 & 0 & 1 & 0 & 0 \\ 0 & 2 & 1 & 0 & 0 & 0 & 0 & 0 \\ 0 & 3 & 1 & 1 & 0 & 1 & 0 & 0 \\ 0 & 3 & 1 & 0 & 0 & 2 & 0 & 0 \\ 0 & 0 & 0 & 0 & 1 & -2 & 0 & 0 \\ 0 & 3 & 1 & 0 & 1 & 0 & 0 & 0 \\ 0 & 2 & 0 & 2 & 1 & 0 & 0 & 1 \\ 0 & 3 & 1 & 0 & 1 & 0 & 1 & 0 \\ 0 & 0 & 0 & 0 & 0 & 0 & 1 & 0 \\ 0 & 0 & 0 & 0 & 0 & 0 & -1 & 0 \\ 0 & 0 & 0 & 0 & 0 & 0 & 0 & 1 \\ 0 & 0 & 0 & 0 & 0 & 0 & 0 & -1 \end{bmatrix} \end{array} \begin{array}{l} N_2(g) \\ O_2(g) \\ CO_2(g) \\ H_2O(g) \\ H_2O \\ H^+ \\ OH^- \\ CO_2 \\ HCO_3^- \\ CO_3^{2-} \\ Ca^{2+} \\ CaCO_3^\circ \\ Ca(OH)_2 \\ CaCO_3 \\ r_2^+ \\ r_2^- \\ r_4^+ \\ r_4^- \end{array} \tag{40}$$

Here, the constraints have been set for the CO_2 in the gas phase and for the $CaCO_3$ precipitate. Both constituents have been shown also as aqueous neutrals. Using conventional notation, the reaction sequence is as follows:

$$Ca(OH)_2(s) \leftrightarrow Ca^{2+}(aq) + 2OH^-(aq) \tag{f.1}$$

$$CO_2(g) \rightarrow CO_2(aq) \tag{f.2}$$

$$CO_2(aq) + 2OH^-(aq) \leftrightarrow CO_3^{2-}(aq) + H_2O \quad \text{(f.3)}$$

$$Ca^{2+}(aq) + CO_3^{2-}(aq) \leftrightarrow CaCO_3(s) \quad \text{(f.4)}$$

When reactions (f.2) and (f.4) are assumed to be the rate-determining steps (re-indexed 2 and 4 in the equations below), it is necessary to define their rate equations which then are applicable in the multiphase model:

$$r_2 = k_2 a\big(CO_2(g)\big)\left[1 - \frac{Q_2}{K_2}\right] \quad (41)$$

$$r_4 = k_4 a(Ca^{2+}) a(CO_3^{2-})\left[1 - \frac{Q_4}{K_4}\right] \quad (42)$$

with the two adjustable rate parameters k_2 and k_4, while all other terms on the right-hand side can again be received from the thermodynamic model. The activities of CO_2(g), Ca^{2+} and CO_3^{2-}, as well as the respective reaction quotients (Q_2 and Q_4), are calculated for each sequential step and thus the discretized model can be based on their subsequent values and the equilibrium constants K_2 and K_4. All other reactions between the constituents defined in matrix (40) are assumed to be in mutual equilibrium in the multiphase model. These fast reactions then necessarily include the reactions between various solute species, which represent the key factors in the pH change to be observed [28, 39]. Typical input data for the system is given in Table 2. The rate constants have been transformed dimensionless by using the residence time of the plug flow reactor. The reaction rate constants were fitted to measured pH data (Fig. 6).

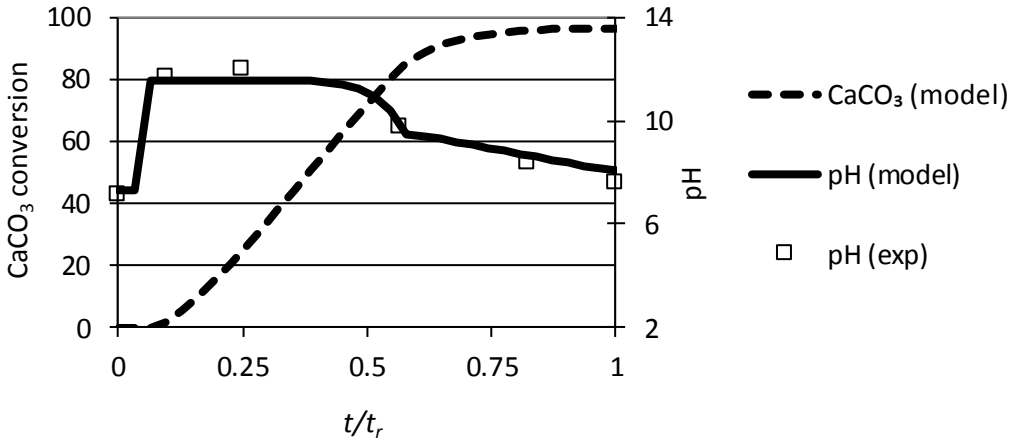

Fig. 6 Modelled and measured pH in the PCC reactor together with the modelled $CaCO_3$ conversion rate as a function of reduced residence time.

Table 2. Typical input data for the lime milk carbonization system.

$Ca(OH)_2$	CO_2	H_2O	*P*	*T*	k_2	k_4
g/s	g/s	l/s	bar	°C		
6.32	3.88	2.04	3.3	50.6	5.7E3	3.5E-3

While the affinities of the equilibrium reactions by definition appear as zero throughout, it is possible to follow again the affinities to the constrained reactions in the multiphase model (Fig. 7). When the affinity of CO_2 dissolution is plotted as a function of affinity of $CaCO_3$ precipitation the various reaction stages can are illustrated visually (Fig. 8). The reaction can be seen to proceed in the affinity space along a path, that for the most part is controlled by relatively simple relationships. Shortly after the injection of both CO_2(g) and $Ca(OH)_2$ slurry, first $CaCO_3$ is formed and both $Ca(OH)_2$

and $CaCO_3$ coexist. Applying the equilibrium assumptions included in the matrix (40), that all the aqueous species are in equilibrium with each other and the dissolution of $Ca(OH)_2$ can be assumed to be in equilibrium as well, the affinity for the precipitation reaction can be expressed as

$$\begin{aligned}\mathbb{A}_2 &= \mu_{CO_2(g)} - \mu_{CO_2(aq)} \\ &= \mu_{CO_2(g)} + \mu_{Ca(OH)_2} - \mu_{CaCO_3} - \mu_{H_2O} - \mathbb{A}_4\end{aligned} \tag{43}$$

When both $Ca(OH)_2$ and $CaCO_3$ coexist with a gas phase of CO_2 with a fixed pressure, while the aqueous phase is dilute enough that water can be considered to have an activity equalling unity, Eq. (43) can be expressed as

$$\begin{aligned}\mathbb{A}_2 &= \Delta G^0\left(CaCO_3(s) + H_2O \rightarrow Ca(OH)_2(s) + CO_2(g)\right) \\ &+ RTln\frac{P_{CO_2}}{P^0} - \mathbb{A}_4\end{aligned} \tag{44}$$

where ΔG^0 is the standard Gibbs energy change for the indicated reaction and P^0 the standard state pressure, so that $\mathbb{A}_2$ is a linear function of $\mathbb{A}_4$. All the other values in Eq. (44) are constants specified by the thermodynamic data of the system and the applied CO_2 pressure. When an excess amount of CO_2 is used, the state of the reactive system will follow the line given by Eq. (44) until all the solid $Ca(OH)_2$ is consumed. System development after that point will depend on the reaction kinetic parameters applied. As an initial asymptotic behaviour after full dissolution of $Ca(OH)_2$, there will be an approximate quasi-steady state relative to aqueous carbonate species in the

system when both the rates (41) and (42) are considerably faster than the net change in aqueous carbonate amount, so that (while both reactions are far from equilibrium)

$$k_2 a\big(CO_2(g)\big) \approx k_4 a(Ca^{2+}) a(CO_3^{2-}) \tag{45}$$

As the aqueous solution coexists with CO_2 gas phase and $CaCO_3$ solid, Eq. (45) can also be written as (K_4 is the equilibrium constant for dissolution of $CaCO_3$)

$$k_2 a\big(CO_2(g)\big) \approx k_4 K_4 \exp\left(\frac{\mathbb{A}_4}{RT}\right) \tag{46}$$

so that the affinity of $CaCO_3$ precipitation is determined by the thermodynamic and kinetic parameters and the CO_2 pressure in the system, not the aqueous composition of the system. This is shown by the vertical dotted line in Fig. 8. After all CO_2 gas has been dissolved, the system state in Fig. 8 moves to the positive x-axis, with a relatively slow $CaCO_3$ precipitation rate. As the inversion point A (where $Ca(OH)_2$ has been fully dissolved) in Fig. 8 and the initial carbonate steady state (vertical line) do not depend on the solution composition, the system had a general tendency after the relatively short reaction time to remain oversaturated in respect to $CaCO_3$ causing scaling after the desired reaction zone. This could be alleviated with the help of the chemical model with a secondary input adjusting the system pH. Due to the reaction pathway as described in **Fig 8**,

the secondary chemical input had to take place after full CO_2 dissolution to be effective.

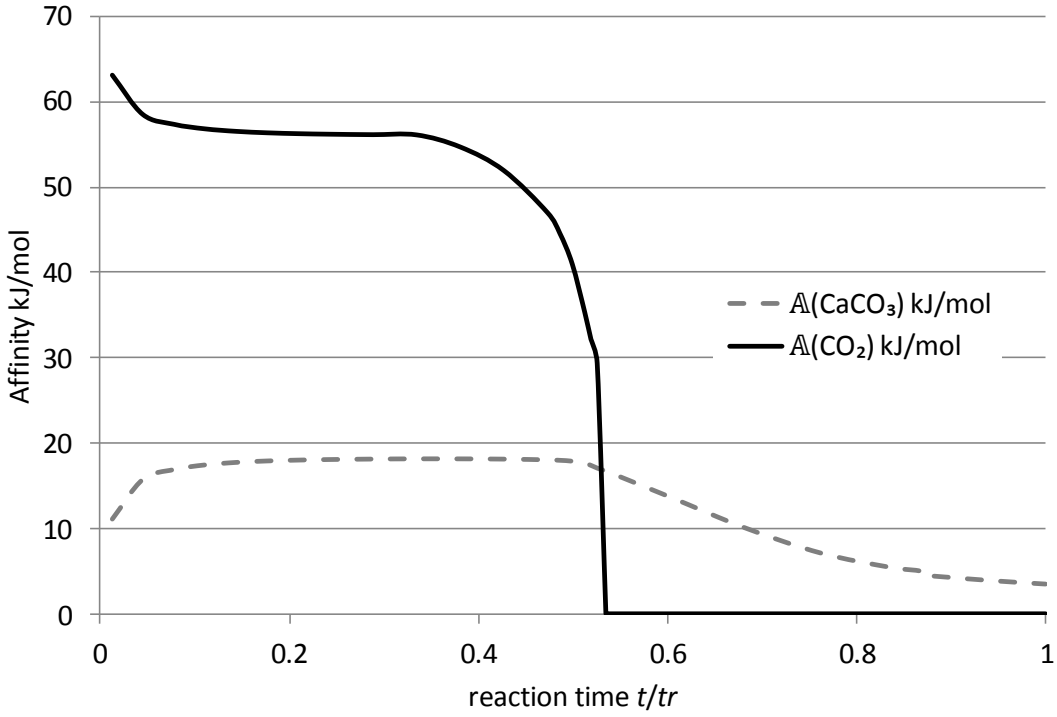

Fig. 7 Reaction affinities as a function of residence time in the PCC reactor.

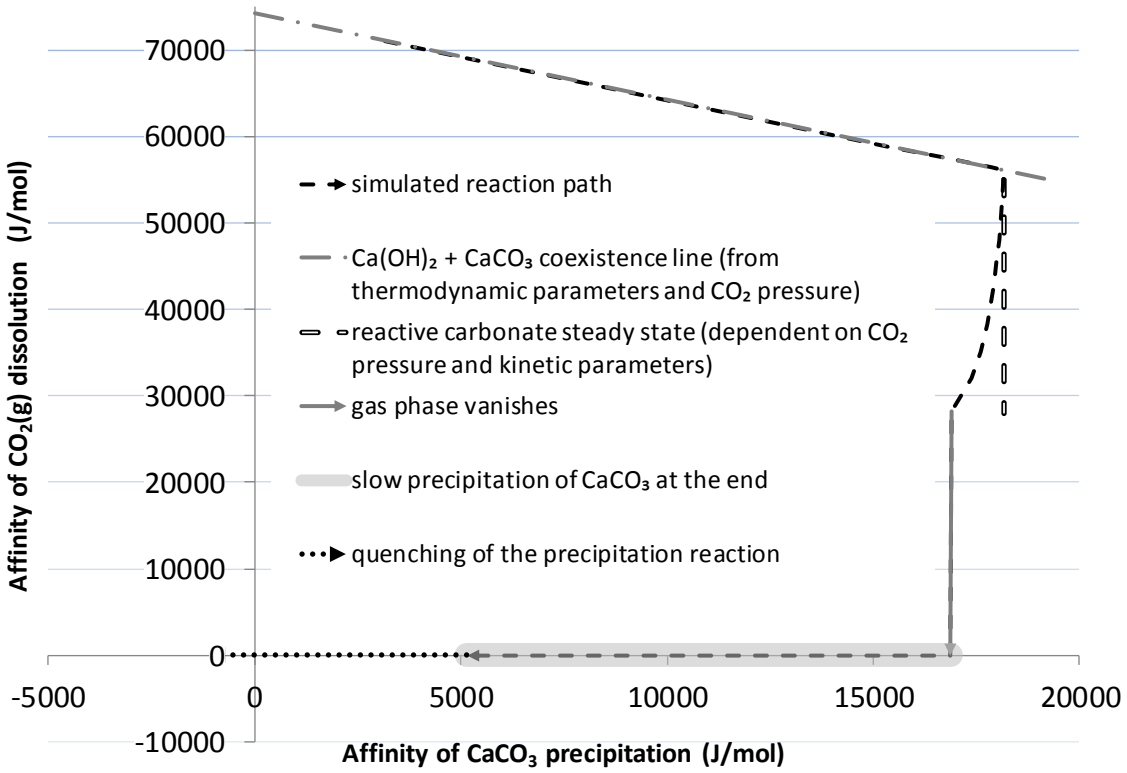

Fig 8. Reaction path in terms of affinities in in the PCC process.

Discussion

The presented methodology allows for systematic and rigorous simulation of various partial equilibria, including those constrained by reaction kinetics, while the assumption of local chemical equilibrium (LCE) is valid for the fast, non-constrained reactions. As indicated by the examples above, the procedure, however, includes a rich chemistry of intermediate species and allows for evaluation of their partial pressures and activities during the course of the chemical change. Then the time-dependent chemical potentials also become defined and affinity of any desired non-equilibrium reaction can

be deduced. Then, it is straightforward to apply the affinity-based reaction rate formalism in the sequential multicomponent calculation. However, it must be emphasized that the rate parameters are not derived from the calculation, but must be given as a program input as gathered, e.g. from experimental data.

The method also provides treatment of, e.g. non-isothermal systems in process modelling as the free energy data will be used as temperature dependent. For chemical reactor engineering, the non-isothermal CFE simulation inherently allows for the effect of the changing temperature on incremental reaction rates. In such calculations, heat exchange between the system (often called the control volume of simulation) and its surroundings is also straightforward to include by using an appropriate heat transfer model or locally measured heat flux rates (e.g. Meyer et al. [40]). In flow systems, the chemical reaction rates must be connected with both mass and heat fluxes (and possible stress factors) and, as a result, the chemical change becomes simulated as a thermodynamic ‘natural process’, and the result of the calculation can be verified to follow the basic laws of thermodynamics.

The affinity received from the constraint potentials can also be interpreted as the driving force while the system is approaching either the equilibrium state or a stable stationary state [25], the latter being a flow system condition where the extensive thermodynamic properties in each

locally positioned element are constant in time and also the intensive quantities at this fixed position remain unchanged over time. However, CFE does not incorporate any specific reference for the stationary state, which is merely defined by the (by experiment) decided rate and flux constraints (Koukkari, 1995; Koukkari and Niemelä, 1997, see also Haase [19]), while the affinities for a non-equilibrium stationary state are determined by the constraint potentials.

As a calculation method, and as presented in the above examples, both CFE, and with it closely related RCCE, can be used as well for transient systems with, e.g. timely changing intensive properties (temperature, pressure, pH or the like). In such conditions the unconstrained 'rest of the system' must be assumed to consist of fast (reaction) processes and it will be even more important than in stationary state calculations to validate the dynamic model by independent measurement.

Conclusion

The constrained free energy method provides a systematic technique to include reaction rates in combination with Gibbs free energy minimization for complex chemical systems. The technique of setting reaction extents as constraints into the multiphase Gibbsian system can be affiliated with the conventional mechanistic approach, where a given subset of the stoichiometric reaction equations is chosen as rate determining steps while

others are assumed to be fast equilibrium reactions. The non-equilibrium affinities ($\mathbb{A}_r$) for individual reactions can then be calculated from the chemical potentials of the constituents (mechanistic and CFE models) or from the constraint potentials (CFE).

While using CFE, the constraint potentials approach zero when the chemical change proceeds toward equilibrium. With constrained reaction rates combined with constrained fluxes (heat and mass transfer) the CFE technique gives the properties of a stationary state. This means the open or continuous system has reached its minimum free energy subject to the said constraints and its thermodynamic extensive properties are constant in time in the positioned element where the local thermodynamic intensive properties also remain unchanged over time. The stationary state calculation is then well defined with its non-zero affinity value, provided that the constraints are adequately set and based on observed kinetic data. Transient systems may also be calculated with the rate-constrained minimum energy approach, yet the validation of the assumptions used with independent experimental data is then even more significant. The particular advantage of the thermochemical method is, however, that it inherently provides a great amount of thermodynamic data. With all extensive and intensive properties of the system under consideration available, there often is a model-

independent measurable property, which can be used to validate the calculations.

Acknowledgements This work was supported by the Strategic Research Council at the Academy of Finland, project Closeloop (grant number 303543).

References

1. Koukkari P, Pajarre R (2006) Calphad 30:18–26.
2. Koukkari P, Pajarre R (2011) Pure Appl Chem 83:1243–1254.
3. Kozeschnik E (2000) Calphad 24:245–252.
4. Pelton AD, Koukkari P, Pajarre R, Eriksson G (2014) J Chem Thermodyn 72:16–22.
5. Pajarre R, Koukkari P, Kangas P (2016) Chem Eng Sci 146:244–258.
6. Koukkari P (1993) Comput Chem Eng 17:1157–1165.
7. Koukkari P, Laukkanen I, Liukkonen S (1997) Fluid Phase Equilib 136:345–362.
8. Keck JC, Gillespie D (1971) Combust Flame 17:237–241.
9. Keck JC (1990) Prog Energy Combust Sci 16:125–154.
10. Janbozorgi M, Ugarte S, Metghalchi H, Keck JC (2009) Combust Flame 156:1871–1885.

11. Ren Z, Goldin GM, Hiremath V, Pope SB (2011) Combust Theory Model 15:827–848.

12. Elbahloul S, Rigopoulos S (2015) Combust Flame 162:2256–2271.

13. De Donder T, Van Rysselberghe P (1936) Thermodynamic theory of affinity. Stanford University Press, Stanford

14. Hillert M (2007) Phase Equilibria, Phase Diagrams and Phase Transformations: Their Thermodynamic Basis, 2nd ed. Cambridge University Press, Cambridge

15. Haase R (1990) Thermodynamics of irreversible processes. Dover, New York

16. Kondepudi D, Prigogine I (1998) Modern Thermodynamics: From Heat Engines to Dissipative Structures. Wiley

17. Kjelstrup S, Bedeaux D, Johannessen E, Gross J (2010) Non-equilibrium Thermodynamics for Engineers. World Scientific, Singapore

18. Ross J, Garcia-Colin LS (1989) J Phys Chem 93:2091–2092.

19. Haase R (1981) Zeitschrift für Phys Chemie 128:225–228.

20. Vuddagiri SR, Hall KR, Eubank PT (2000) Ind Eng Chem Res 39:508–517.

21. Lems S, van der Kooi H., de Swaan Arons J (2003) Chem Eng Sci 58:2001–2009.

22. Qian H, Beard D a. (2005) Biophys Chem 114:213–220.

23. Bordel S, Nielsen J (2010) Metab Eng 12:369–377.

24. Niven RK (2010) Philos Trans R Soc B Biol Sci 365:1323–1331.

25. Ross J, Corlan AD, Müller SC (2012) J Phys Chem B 116:7858–65.

26. Smith WR, Missen RW (1991) Chemical Reaction Equilibrium Analysis: Theory and Algorithms. Krieger publishing company, Malabar, Florida

27. Koukkari P (1995) A physico-chemical reactor calculation by successive stationary states. Dissertation, Helsinki University of Technology

28. Koukkari P, Pajarre R, Blomberg PBA (2011) Pure Appl Chem 83:1063–1074.

29. Kangas P, Koukkari P, Brink A, Hupa M (2015) Chem Eng Technol 38:1173–1182.

30. Kangas P, Vidal Vázquez F, Savolainen J, et al (2017) Fuel 197:217–225.

31. Blomberg PBA, Koukkari P (2011) Comput Chem Eng 35:1238–1250.

32. Cheluget EL, Missen RW, Smith WR (1987) J Phys Chem 91:2428–2432.

33. Norval GW, Phillips MJ, Missen RW, Smith WR (1991) Can J Chem Eng 69:1184–1192.

34. Koukkari P, Niemelä J (1997) Comput Chem Eng 21:245–253.

35. West RH, Celnik MS, Inderwildi OR, et al (2007) Ind Eng Chem Res 46:6147–6156.

36. Koukkari P, Penttilä K, Keegel M (2000) Coupled Thermodynamic and Kinetic Models for High-Temperature Processes. In: Proc. 10th Int. IUPAC Conf. High Temp. Mater. Chem. Forscungszentrum Julich, pp 253–256

37. Coda Zabetta E, Hupa M (2008) Combust Flame 152:14–27.

38. Zeldovich J (1946) The Oxidation of Nitrogen in Combustion and Explosions. Acta Physicochim URSS XXI:577–628.

39. Koukkari P (2010) ChemSheet Model for the Direct Carbonation of Lime Milk in an Integrated PCC Process. In: Paperitehdaspäivät. Savonlinna, p P5

40. Meyer V, Pisch A, Penttilä K, Koukkari P (2016) Chem Eng Res Des 115:335–347.

Figure Captions

Fig. 1 The constraint potential affinities and $\Delta_r G$ values for the SO_2 oxidation system

Fig. 2 The constraint potential affinities and $\Delta_r G$ values for the isothermal $TiCl_4$ oxidation system.

Fig. 3 The constraint potential affinities and $\Delta_r G$ values for the non-isothermal TiCl4 oxidation system.

Fig. 4 Comparison of the CFE and DKM calculation results for the NO formation model.

Fig. 5 Evolution of reaction affinities during the NO formation model.

Fig. 6 Modelled and measured pH in the PCC reactor together with modelled $CaCO_3$ conversion rate as function of reduced residence time.

Fig. 7 Reaction affinities as a function of residence time in the PCC reactor.

Fig. 8 Reaction path in terms of affinities in in the PCC process.

Table 1 The rate data for the SO2 and TiCl4 oxidation reactions.

Reaction	ΔH^o kJ · mol^{-1}	ΔG^o kJ · mol^{-1}	Rate equation	E_a kJ · mol^{-1}	A s^{-1}	A' (dm^3 · mol^{-1})^{½}s^{-1}
$SO_2 + 0.5O_2 \rightarrow SO_3$	-98.9	-35.5	$\frac{d[SO_3]}{dt} = k[O_2][SO_2]$	31.0	12.07	
$TiCl_4 + O_2 \rightarrow TiO_2 + 2Cl_2$	-175.4 (1000 °C)	-104.1 (1000 °C)	$\frac{d[TiCL_4]}{dt} = -\left(k + k'\sqrt{[O_2]}\right)[TiCl_4]$	85.0	8.26E4	1.4E5

Table 2 Typical input data for the lime milk carbonization system.

$Ca(OH)_2$	CO_2	H_2O	P	T	k_2	k_4
g/s	g/s	l/s	bar	°C		
6.32	3.88	2.04	3.3	50.6	5.7E3	3.5E-3

Figure 1

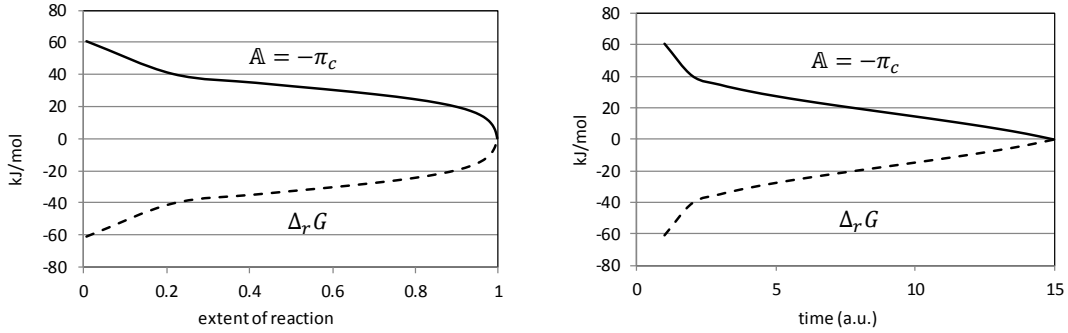

Figure 2

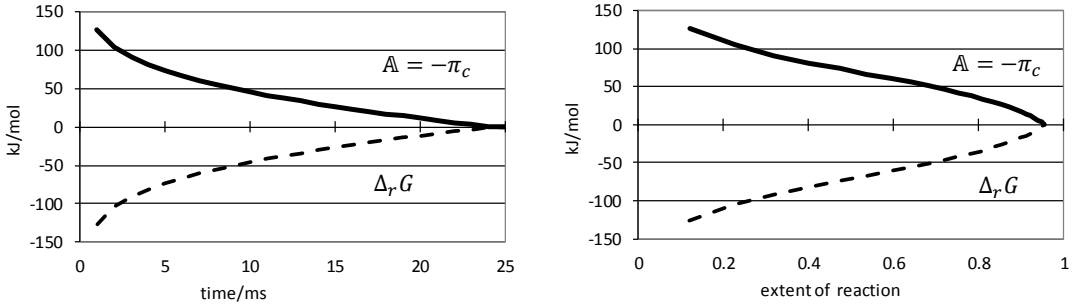

Figure 3

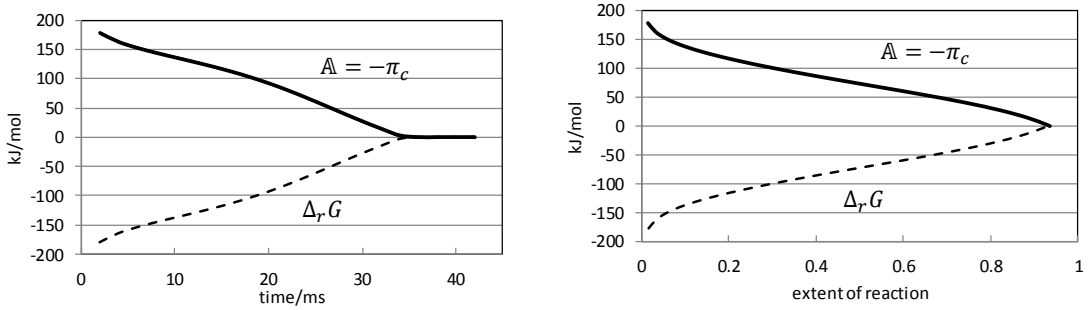

1 *Figure 4*

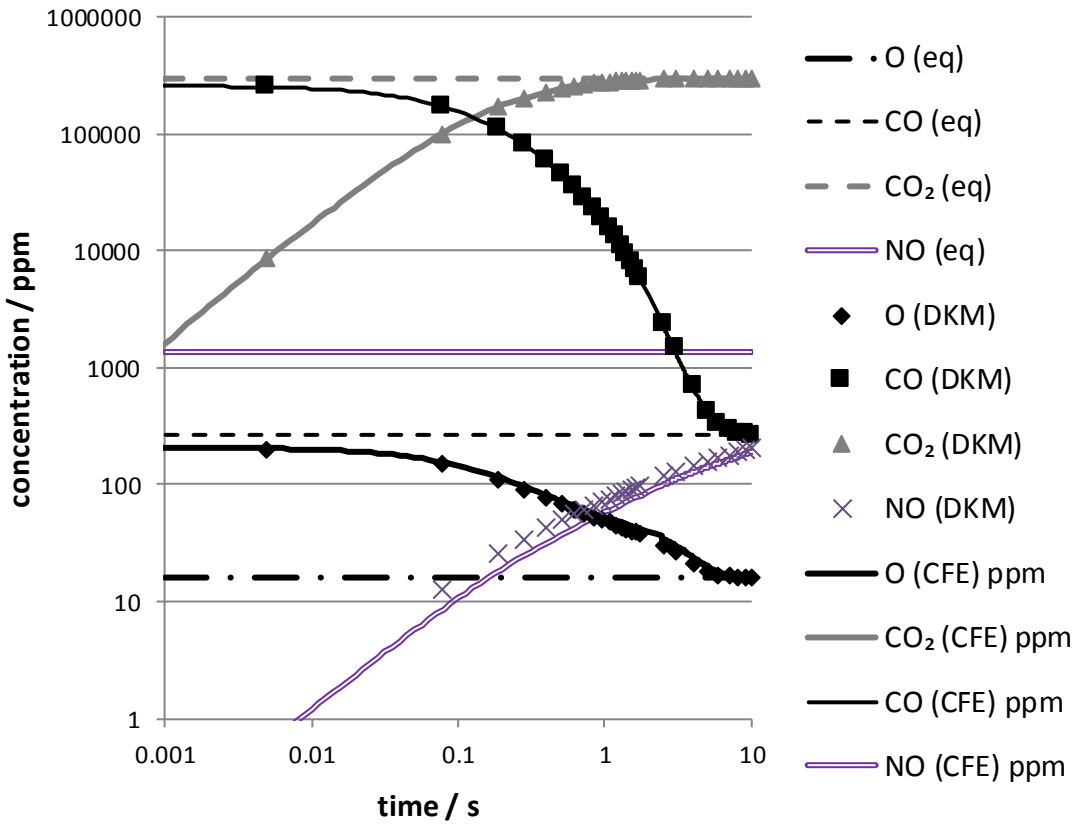

2

3 *Figure 5*

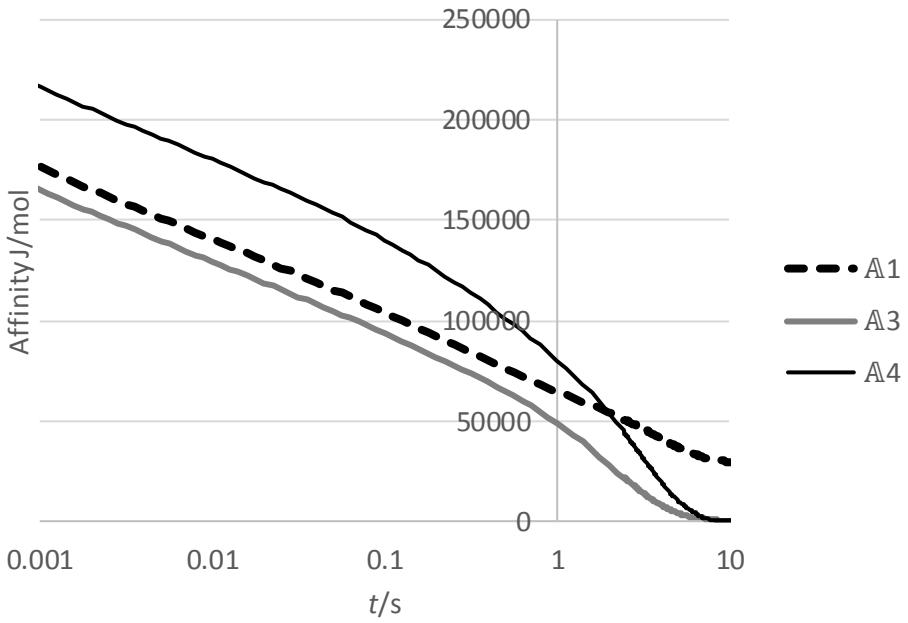

4

1 *Figure 6*

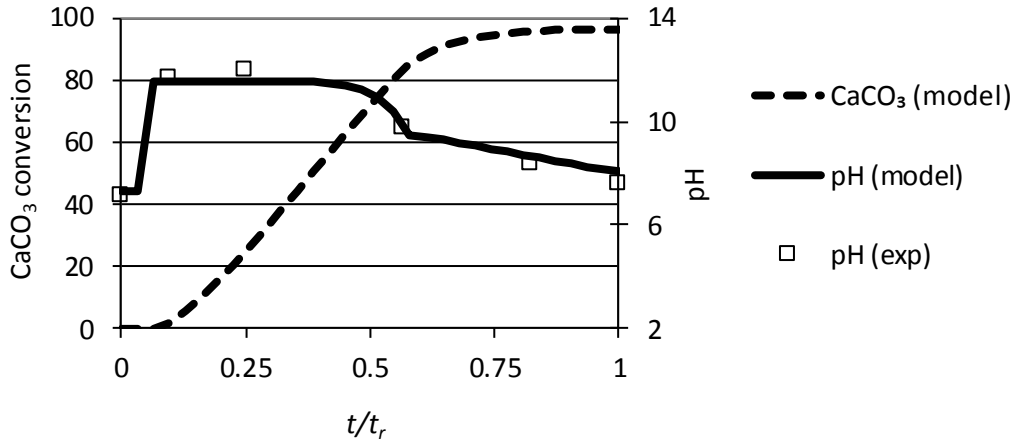

2

3 *Figure 7*

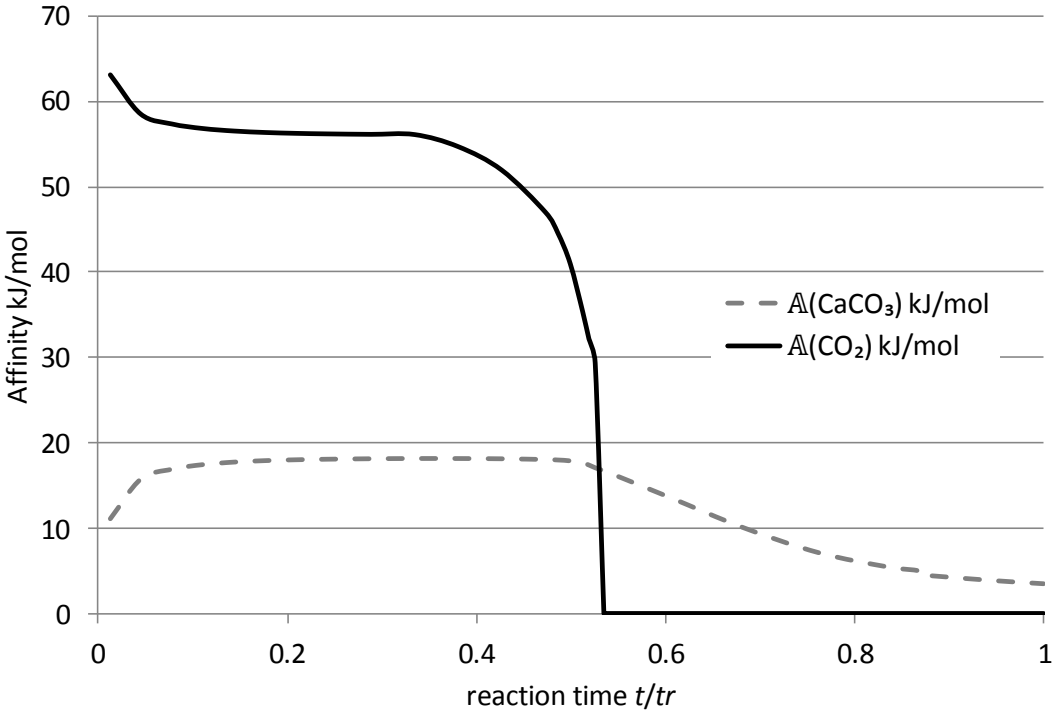

4

5

6

7

8

Figure 8

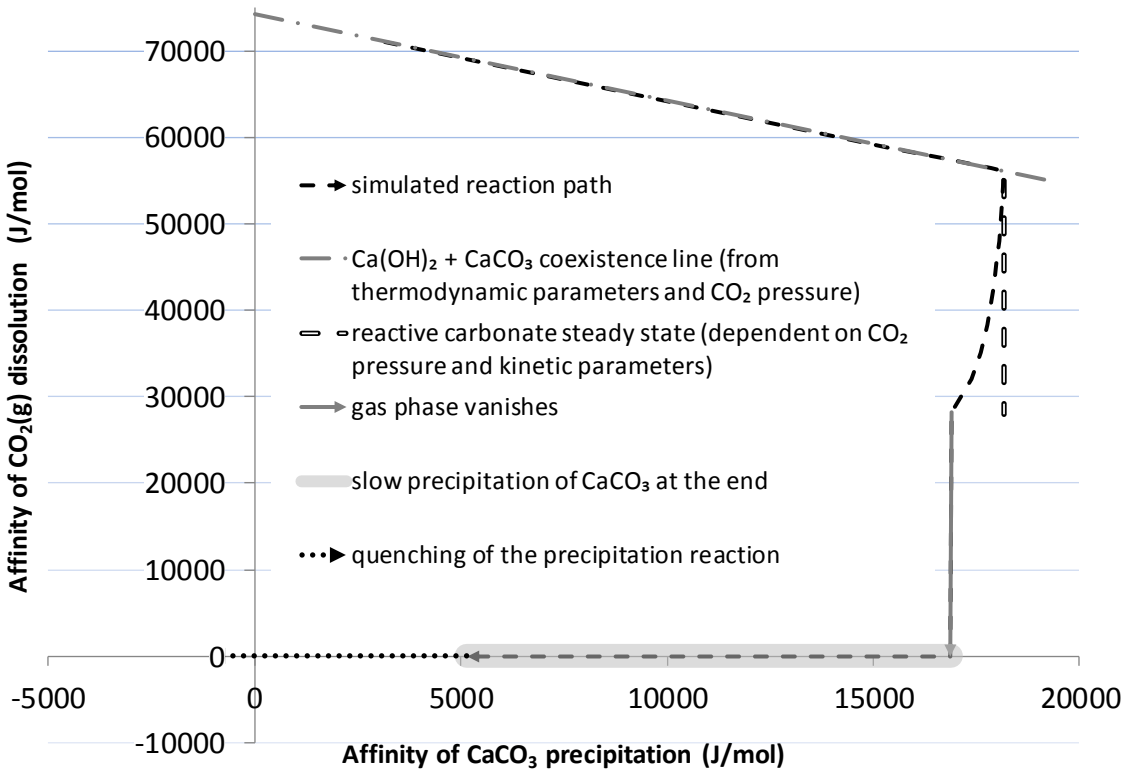
70000
60000
50000
40000
30000
20000
10000
0
-10000
-5000
0
5000
10000
15000
20000
Affinity of CO_2(g) dissolution (J/mol)
Affinity of $CaCO_3$ precipitation (J/mol)
simulated reaction path
$Ca(OH)_2$ + $CaCO_3$ coexistence line (from thermodynamic parameters and CO_2 pressure)
reactive carbonate steady state (dependent on CO_2 pressure and kinetic parameters)
gas phase vanishes
slow precipitation of $CaCO_3$ at the end
quenching of the precipitation reaction